Stochastic simulation algorithms for beta-amyloid aggregation in Alzheimer Disease

Network Modeling and Simulation course report

Carlo Aleotti, Anastasia Santo, Rayan Slatni

January 2024

Abstract

In our project we performed some exploitative analysis trying to continue the work done in [1] about beta-amyloid filaments aggregation. We developed some stochastic algorithms in order to simulate the aggregation of the beta-amyloid protein, focusing on the case of Alzheimer disease. We conducted simulations with stochastic algorithms (Gillespie, DM, FRM), implementing customized versions for the model provided by[1] in order to simulate the aggregation mechanism of beta-amyloid proteins. As proposed by [1] we used Monte Carlo method on top of our stochastic simulation algorithms to average out the results and reduce any anomalies that may be present in a single simulation to obtain an average of the results. These simulations were performed using different initial conditions and different reaction rates (as provided by[1]). We also used the software HSimulator for the hybrid HRSSA algorithm provided by[9] to obtain further evidence of the system dynamics. Furthermore, we looked at the stability of the equilibria, trying to obtain additional information about the protein aggregation, and we then hypothesized a possible mechanism for optimizing the parameters related to the reactions of the model.

Introduction

In neurophysiological conditions the APP (Amyloid Protein Precursor), a trans-membrane receptor that plays important roles in brain homeostasis, is cleaved by a beta-secretase leading to the formation of beta-amyloid protein, which is in fact a proteolytic product of APP[7]. The Aβ peptides are generate with a predominance of of the 40 aminoacidic form (Aβ40) followed by 42 aminoacidic form (Aβ42), which is more prone to aggregation. In Alzheimer Disease (AD) this pathway is slightly modified, in fact some genetic mutation in APP gene (or associated genes) can lead to an over expression of beta-amyloid and a reduction of its clearance, resulting in an accumulation of this protein[4]. When present in high concentrations this protein tends to undergo conformational changes leading to a beta-sheet structure, which if in a solution tend to stabilize through polymerization reactions leading to the formation of fibrils that aggregate into plaques[8]. Under the *amyloid hypothesis* this plaques are linked to the cognitive decline that we observe in AD, caused by their cellular toxicity [10]. The mechanism juts described is AD specific, but the aggregation of proteins is observed in several neurodegenerative disease[11]. In Fig.1 are schematize the dynamics of polymerization. The soluble monomers of length 1 (M_1) correspond to APP and are the population of free protein $m(t)$, then they aggregate in β-amyloid filaments of length i (M_i). The formation of oligomers is driven by the primary nucleation (reaction rate K_n), the oligomers are thermodynamically unstable[8] so through the elongation (K_+) a filaments M_i is formed. The main objective of the work of [1] is to use the mathematical and computational framework to unravel the stochastic nature of the elongation, propagation and possible fragmentation of Aβ peptides. They treat this process as a chemical reaction process and use the chemical kinetics of the intricate reaction, which is responsible for forming the filamentous protein structure. Hence Stochastic Modeling can be used to understand the progression of Amyloid-Beta Aggregation which eventually leads to larger plaques

formation and development of Alzheimer disease in patients. These filaments are the most toxic structure and need attention for both understanding the disease and deriving the potential cure.

Mathematical Theory

The linear growth of filaments initiated by a primary nucleation reaction is formalized in Oosawa's theory[16]. The initial association of monomers is generally considered to be thermodynamically unfavorable due to free energy barrier, on the other hand the subsequent addition of monomers or oligomers to the fibrils is thermodynamically favorable[6]. Other reactions are the dissociation (K_{off}) of M_1, fragmentation (K_-) and aggregation (K_+) of already formed filaments, and the monomer-dependent secondary nucleation (K_2). Monomer-dependent secondary nucleation is defined as a process whereby nucleus formation from monomers (M_2) is catalysed by existing aggregates composed of the same type of monomeric building blocks. Usually this takes the form of monomers forming a nucleus on the surface of an already existing aggregate[13]. The law of mass action serves as the foundation for robust kinetic models that effectively define the chemical kinetics of intricate reaction networks controlling the growth of filamentous protein structures.[1]. The mathematical theory behind modeling chemical reactions networks with stochastic processes involves the use of the chemical master equation, which describes the time evolution of the probability distribution of the state of a chemical system. The chemical master equation can be derived from the principle of detailed balance, which states that the rate of each reaction is balanced by the reverse reaction, ensuring that the system is in a state of equilibrium. The reaction kinetics can be formalized as:

$$s_{ji}X_i + \ldots + r_{jn}X_n \tag{1}$$

where $i = 1, .., n$ number of species, $j = 1, .., M$ number of reactions, $S_{ji} = r_{ji} - s_{ji}$ is the stoichiometric matrix. The five reactions that define the system are summarized in a table 1. Under well-mixed and dilute conditions, if $P(x, t)$ denotes the probability for the state vector $x(t) = x_1, ..., x_n$ at time t, then the probability evolution of the system (1) can be described by chemical master equation in the stochastic framework:

$$\frac{dP(x,t)}{dt} = \sum_{j=1}^{M} P(x - S_j, t)a_j(x - S_j) \quad - \sum_{j=1}^{M} P(x,t)a_j(x) \tag{2}$$

where S_j is the row vector of the stoichiometric matrix and $a_j(x)$ is the propensity function[1]. In a deterministic setting [14],[5] established master equations together with the criterion for primary nucleation, elongation and other secondary events (secondary nucleation, fragmentation and monomer-dependent elongation), which was derived based on the kinetics of these microscopic processes and their impact on the concentration changes of chains of length j over time, represented by $f(t, j)$:

$$\frac{df(t,i)}{dt} = 2m(t)k + f(t, j-1) - 2m(t)k + f(t,j) + 2m(t)k_{\text{off}}f(t, j+1) - 2m(t)k_{\text{off}}f(t,j) \tag{3}$$

$$- k_-(j-1)f(t,j) + 2k_- \sum_{i=j=1}^{\infty} f(t,i) + k_2 m(t)_2^n \sum_{i=j=1}^{\infty} if(t,i)\delta_{j,n2}k_n m(t)^n c\delta_{j,n2} \tag{4}$$

The quantity $f(t, j)$ denotes the number of aggregates made up of j units that are found at time t. $m(t)$ is the temporal variation of the free monomer concentration, n_c is the critical nucleus size. The equation describes the primary nucleation (k_n), the elongation process ($k+$), accounts for dissociation reactions ($k-$), fragmentation (k_{off}) and primary nucleation (k_2) [12]. Note that $j \geq n_c$ because we are assuming that aggregates with a length of $1 < j < n_c$ are unstable so that they either move on to aggregate or break

into monomers rapidly[3]. The temporal variation of the free monomer concentration $m(t)$ is defined as[3]:

$$dm(t)/dt = -d/dt \sum_{j=nc}^{\infty} jf(t,j) \tag{5}$$

Several approximation schemes have been proposed to solve the deterministic equation analytically, among these methods, the method of principal moments is the most commonly used. The zeroth principal moment, $P(t) = \sum_{j=nc}^{\infty} f(t,j)$, is the total number of aggregates in the system, and the first principal moment, $M(t) = \sum_{j=nc}^{\infty} jf(t,j)$, represents the total mass concentration of the aggregated monomers (the fibril mass)[3]. The ODEs of $P(t)$ and $M(t)$ are defined later in equations 6 and 7.
In [5] they established another chemical master equation to capture the stochastic effects in early amyloid aggregation to describe the aggregation of monomers into oligomers, hence that describes the evolution of the system. They used log-normal closure moment method rather than direct simulations. In [1] analysis of filaments up to length eight, the chemical master equation for the model is formulated as outlined in [5]. Free proteins are denoted free as M1; specifically, $x1, x2, x3, x4, x5, x6, x7$ and $x8$ correspond to filaments up to length eight ($M1$ to $M8$). Given the substantial number of constants involved in total—during the modeling of both the aggregation and fragmentation (the complete kinetics are provided in Tables S1 and S2 of the Supplementary Material), our analysis primarily centers on stochastic simulations. We refrain from explicitly delving into the numerical solutions of the master equation, keeping our focus squarely on the stochastic simulation.

Chemical Reactions	Reaction Rate	Explanation
$M_1 + M_1 \rightarrow M_2$	k_n	Primary Nucleation
$M_i + M_1 \rightarrow M_{i+1}$	k_+	Elongation, $i \geq 2$
$M_i + M_1 \leftarrow M_{i+1}$	k_{off}	Dissociation, $i \geq 2$
$M_i + M_j \rightarrow M_{i+j}$	k_+	Aggregation, $2 \leq i < \infty$
$M_i + M_j \leftarrow M_{i+j}$	k_-	Fragmentation, $2 \leq i < \infty, 2 \leq j \leq i$

Table 1: *System's reaction*

Methods

In order to understand the progression of amyloid-beta aggregation we followed the pipeline proposed in[1]: the progression of filaments is treated as a stochastic chemical reaction process in order to understand the inherent randomness and complex spatial–temporal features of the system. In the model development we considered the following assumptions:

1. Amyloid Hypothesis;
2. The progression of filaments was simulated up to length 8, otherwise it will become computationally expensive;
3. Spatial Homogeneity;
4. Constant monomer concentration in order to obtain the closed form early time solution[3].

After developing the model, one for aggregation only, one for aggregation and secondary events, they performed Gillespie[15] algorithm simulations to simulate the aggregation and fragmentation processes, and used Monte Carlo algorithm to average out the results and reduce any anomalies that may be present in a single simulation[1]. Gillespie algorithm lies on randomly picking up the next reaction time, and the next reaction event that can occur from the set of possible events[1].
Our main contribution lies in conducting detailed simulations and reaction kinetics analyses to understand the stochastic nature of amyloid-beta aggregation, which includes experimenting with various reaction

propensities and initial conditions (as fixed in [1]). The random switch of propensity proposed in the paper[1] was not simulated because it does not significantly alter the dominance of certain reaction events in the overall dynamic Fig.10, and in the mean time it was already shown how the extent of random switching was directly proportional to the extent of change in convergence. Details about the initial conditions and the reaction rates are provided in the result section.
In addition to the Monte Carlo-Gillespie algorithm proposed in the paper[1], we tried other algorithm implementations to see if we could improve the their work. In particular we execute: First Reaction Method (FRM), the Direct Method as studied in class(DM), and HRSSA. The code for FRM, DM and and the Monte Carlo-Gillespie is provided in the matlab script (Matlab version Version 23.2 (R2023b)[2]), instead HRSSA was implemented using the software HSimulator[9].
Secondly, as suggested in[1] we tried to perform a stability analysis of the system, with the aim of founding the equilibria points of the system of equations (6 and 7), study their stability and try to infer some information about the behaviour of beta-amyloid aggregation.

Results

Simulation results

Firstly we tried to reproduce the simulation presented in the paper[1] using Monte Carlo-Gillespie with the same parameters conditions that they proposed. In particular we tried different set of reaction rates $(k_0, ..., k_{53})$, different initial population size $(M1 = 10000 and M2 = 5000)$, and different intermediate populations size because it may be possible that in the reaction's environment the initial population of other species $(M2, ..., M8)$ is not exactly zero at the beginning of the dynamics. We focused on the five following implementation:

1. Aggregation-only model with different rate constants for each reaction $(k_0 \neq \ldots \neq k_{53})$, setting $k_0 = 0.00001$, $k_1 = k_0/2, \ldots$, testing two initial populations of free protein $M_1 = 10000$ and $M_1 = 5000$, and the other populations $M_2, \ldots, M_8$ are respectively $100, 60, 50, 20, 10, 5, 5$ Fig.2, Fig.3.

2. Same as 1), but the other populations $M_2, \ldots, M_8 = 1$ (Supp.Fig1 and Fig2).

3. Aggregation and fragmentation model with different rate constants for each reaction ($(k_0 \neq \ldots \neq k_{53})$, setting starting reaction rate for aggregation $(k_0 = k_1 = 0.00001)$, and for fragmentation $(k_1 = k_0/2, \ldots)$, while all the other constants are calculate as $(k_2 = k_0/2, k_3 = k_1/2)$; testing two initial populations of free protein $M_1 = 10000$ and $M_1 = 5000$, and the other populations $M_2, \ldots, M_8 = 100$ Fig.4, Fig.5.

4. Same as 3), but the other populations $M_2, \ldots, M_8 = 1$.

5. Same as 3), but only with three constant reaction rates: $k_0 = 0.00001$, $k_1 = \ldots = k_{26} = 0.0000000002$, and $k_{27} = \ldots = k_{53} = k_1/2$, Fig.6, Fig.7.

First of all it appears clear how varying the initial populations of M1 result in distinct convergence patterns. Notably, it appears clear that higher the value of M1, higher the number of filaments of length from 5 to 8; Looking even to the initial population size of the oligomers in the different plots [1] it seems that there is a nonlinear relationship between the initial population sizes and system behavior, suggesting a threshold effect, where beyond a certain population size, the system dynamics alter significantly. Comparing Fig.2 Fig.3 with the conditions 2(Supp.Fig1 and Fig2), there is a difference in M_3 and M_4 due to the different starting point, in the others the starting points are too close to see any differences, but overall the dynamics with same reaction rates and different population size are almost the same. The same happens when comparing condition 1 (Fig.2, 3) and 3 in Fig.4, 5 leading to the conclusion that

adding the fragmentation events to the system doesn't influence a lot the dynamics, indeed the primary nucleation is the event that in average account for the majority variability of the system (as shown in Fig.8 from [1]). The major difference is seen in Fig.6, 7, where the reaction rates are chosen in a different way. M_1 in this case decreases slower and the other filaments have distinct behavior. Then we can see that the standard deviation in Fig.4, 5 are generally (except for M5 and M7) larger than in Fig.6, 7, because we are using just three different reaction rates. In Fig.5 the M6 density has an horizontal asymptote while in the other case it keep increase. Lastly we note that in M8 in Fig.7 the two populations overlap at the end on the dynamic. Between the conditions 3 and 4, where only the population size is different, the only filaments that change the behaviour are M3 (Supp.Fig7) and M8, in fact in Supp.Fig8 we can see that the difference in the initial population size 10000 or 5000 is very slight respect to 5. From Fig.10, it is clear that certain reaction events dominate the overall dynamics of the process. This observation is critical in understanding the inherent behavior of the system under study. Furthermore, as said before, the introduction of random switching of probabilities does not significantly alter the dominance of certain reaction events in the overall dynamics. This observation indicates that, despite the random elements introduced in the reaction propensities, the core characteristics of the process are largely maintained, while without the random switching of the probabilities, the dynamics tend to aggregate more filaments of different lengths than in the case of using the random switching of probabilities (Fig.11).

Zero and First Moment

Since the dynamics can be summarized using the zero and first moment, respectively polymer number and polymer mass concentration, we report their time evolution and their ration that correspond to the average length of filaments, defined below as:

$$AverageLength = \frac{M(t)}{P(t)}$$

We decide to focus on the dynamics with condition 3)(Fig.8) and 5)(Fig.9) since are the ones that highlighted the main differences due to the different propensities setting. We can see that in both cases the first moment $M(t)$ is always positive, meaning that the polymer mass concentration never decrease over time. The only differences is in the velocity of the growth: in Fig.9 the reaction the rate $k1$ is smaller leading to a smaller time derivative so the slope is less steep in the first half of the dynamics (till $time = 500$). About the zero moment $P(t)$ in Fig.9 at the very beginning we can see a slight decrease of the polymer number. This can be explained by the fact that at the beginning ($t \approx 0$) the only reaction firing is the oligomerization into M_2, since this step is thermodynamically limited can lead only to a decrease in the number of filaments because they can only aggregate. After some time ($t > 50$) we observe both aggregation and fragmentation leading overall to an augment of the filament number. Instead in Fig.8 we can only observe the $P(t)$ increasing because the reaction rate are higher and so the reaction fires quickly. About the average length of filaments we observe that the length M_8 is never reached meaning that even if the filament tend to aggregate together, there is always a small portion of reactions that fragment the filaments. In particular in Fig.9 we observe an average of 6.5, while in Fig.8 we have 5.8. This might be reasonable because in Fig.8 the reaction propensity (both for aggregation and fragmentation) is in the order of 10^{-14} and in the other case is 10^{-10}.

Algorithms performance

The performance of the algorithms implemented (Monte Carlo-Gillespie from[1], FRM and DM) was evaluated using profiling. Profiling is a way to measure the time it takes to run code in MATlab and identify where it spends the most time. In particular it tells us which functions are consuming the most time, so we can evaluate them for possible performance improvements. In our case profiling provides detailed information on the execution time of each simulation implemented, allowing us to select the most efficient one. We evaluated the time performance of Monte Carlo for three different simulations

Algorithms: FRM, Gillespie from the paper pseudo-code and DM. We saw that for the easiest model of aggregation-only (condition 3) the DM Algorithm is the one that consumes the least times (26.904s), compared to Gillespie (44.329s), and we selected it in order to perform all the simulations in the most efficient way. The profiling results can be found in the supplementary material (Fig.3,4).
A limitation highlighted by the authors[1] is related to the absence of realistic numbers of soluble protein extended-duration simulations; indeed, longer simulations could offer a more realistic representation of the studied biological processes. To achieve this, adequate computational resources and techniques are needed, and we found the idea of trying a hybrid HRSSA algorithm interesting for two reasons: first of all, it proves to be computationally very efficient (often faster than COPASI[9]), which could allow for lower computational costs for more realistic simulations. Secondly, the authors of the paper[1] highlight a statistically consistent pattern, with primary nucleation, elongation, and aggregation with monomer-dependent secondary nucleation being the most frequent reaction events. This consistency reveals an underlying determinism in the system, so the HRSSA algorithm seems suitable for the type of situation presented by our model: some very fast reactions with very high propensities, and other reactions where the stochastic component is predominant and require longer times to manifest their effects.
After the previous simulations, we tried to simulate the system with and hybrid simulation algorithm[9]: the idea came from the fact that the primary nucleation and the secondary nucleation have higher propensities than the others. So we used the HRSSA and it improved the algorithm. In Fig.12 and Fig.13 we can see the different decreasing of M1, in fact with lower reaction rate the decreasing of monomers is slower. We can also notice that M6 in Fig.12 reaches a plateau but in the other case is the growth is continuous, suggesting that a length of 6 monomer might a good average between the aggregation/fragmentation events.

Stability Analysis

Firstly, we analyzed system's stability and convergence, as suggested by the article[1]. We have 2 non linear ordinary differential equations:

$$\frac{dP}{dt} = k_-[M(t) - (2n_c - 1)P(t)] + \quad +k_2 m(t)^{n_2} M(t) + k_n m(t)^{n_c} \tag{6}$$

and

$$\frac{dM}{dt} = 2[m(t)k_+ - k_{off} - k_- n_c(n_c - 1)/2]P(t) + n_2 k_2 m(t)^{n_2} M(t) + n_c k_n m(t)^{n_c} \tag{7}$$

we computed the equilibria obtaining:

$$P(t) = M(t)\left(\frac{1}{2n_c - 1} + \frac{k_2 m(t)^{n_2}}{k_-(2n_c - 1)}\right) + \frac{k_n m(t)^{n_c}}{k_-(2n_c - 1)} \tag{8}$$

and

$$M(t) = \frac{-2k_+k_n m(t)^{n_c+1} + 2k_{off}k_n m(t)^{n_c} + 2n_c(n_c-1)k_-k_n m(t)^{n_c} - k_-(2n_c-1)n_c k_n m}{2k_-k_+ m(t) + 2k_2k_+ m(t)^{n_2+1} - 2k_{off}k_- - 2k_{off}k_2 m(t)^{n_2} - k_-^2 n_c(n_c-1) - k_2k_-n_c(n_c-1) - k_2k_-n_c(n_c-1)} \tag{9}$$

At this point, was difficult to study the stability of the equilibrium, because of the non linearity, so we tried to see an easier situation than the one before via simplify the system neglecting the firing of

secondary nucleation reactions ($k_2 = 0$) as done in[12]; doing the same computation. So the equations became:

$$\frac{dP_0}{dt} = k_-[M_0(t) - (2n_c - 1)P_0(t)] + k_n m(0)^{n_c} \tag{10}$$

and

$$\frac{dM_0}{dt} = 2[m(0)k_+ - k_{off} - k_- n_c(n_c - 1)/2]P_0(t) + n_c k_n m(0)^{n_c} \tag{11}$$

obtaining the equilibrium:

$$P_0(t) = \frac{-n_c k_n m(0)^{n_c}}{2[m(0)k_+ - k_{off} - k_-(n_c - 1)/2]} \tag{12}$$

and

$$M_0(t) = -\frac{k_n}{k_-} + \frac{-(2n_c - 1)n_c k_n m(0)^{n_c}}{2[m(0)k_+ - k_{off} - k_-(n_c - 1)/2]} \tag{13}$$

and the Jacobian matrix at the equilibrium:

$$J = \begin{pmatrix} 0 & 2[m(0)k_+ - k_{off} - k_- n_c(n_c - 1)/2] \\ k_- & -k_-(2n_c - 1) \end{pmatrix}$$

with determinant and trace:

$$detJ = 2k_-[m(0)k_+ - k_{off} - k_- n_c(n_c - 1)/2] \tag{14}$$

$$trJ = -k_-(2n_c - 1) \tag{15}$$

Since the determinant is positive and the trace is negative, the equilibrium computed assuming the simplification $k_2 = 0$ is asymptotically stable.
Again, as suggested by the authors of the paper, we tried to see if, from a qualitative analysis of the equations, there's a threshold effect between the initial population size

$$m(0)$$

and the system behavior. We didn't find anything analytically, but maybe, changing the value of the initial population given some experimental data and doing several simulations, it's realistic to determine that threshold.

Conclusion

Through this work we tried to simulate the system dynamics of beta-amyloid protein using stochastic simulation algorithms and to performe a study of the equilibria looking for the stability of the system.
About the stability the main issue was the computation itself since the system was non-linear, therefore we tried a simplified version excluding the secondary nucleation reactions. In this way we found a stable equilibrium, but we can't generalized for the complete system. About the algorithm we saw that DM could be a better implementation of the standard Gillespie used in the paper because the computational

time is reduced. Using the hybrid version (HRSSA) we allow to take into account the fact that the primary nucleation dominate the system dynamics, obtaining better computational result. We decided to don't implement deterministic simulation because (as already pointed out in [1]) they can not capture the inherent stochastic nature present in the bio-chemical reactions. The main observations are: the predominance of the primary nucleation over the other system reactions, the convergence towards filaments of length 6, and the sensitivity of the system to the propensities choice.
Further improvement can include the use of experimental data to develop an optimization strategy for the parameter estimation of the reaction rates.

References

[1] V.P. et. al Ojha. "Stochastic Modeling and Simulation of Filament Aggregation in Alzheimer's Disease". In: *Processes* (2024). DOI: 10.3390/pr12010157.

[2] "The MathWorks Inc. (2023) Natick, Massachusetts: The MathWorks Inc. https://www.mathworks.com". In: (2023).

[3] et. al Jia-Liang Shen. "Modeling Protein Aggregation Kinetics: The Method of Second Stochasticization". In: *The Journal of Physical Chemistry* (2021). DOI: 10.1021/acs.jpcb.0c10331.

[4] T Guo. "Molecular and cellular mechanisms underlying the pathogenesis of Alzheimer's disease". In: *Mol Neurodegeneration* (2020). DOI: 10.1186/s13024-020-00391-7.

[5] R.N et. al Liu. "Stochastic master equation for early protein aggregation in the transthyretin amyloid disease". In: *Nature* (2020). DOI: 10.1038/s41598-020-69319-x.

[6] at. al B. Morel. "Early mechanisms of amyloid fibril nucleation in model and disease-related proteins". In: *ScienceDirect* (2019). DOI: 10.1016/j.bbapap.2019.140264.

[7] et. al Xu-Qiao Chen. "Alzheimer Disease Pathogenesis: Insights From Molecular and Cellular Biology Studies of Oligomeric A and Tau Species". In: *Frontiers* (2019). DOI: 10.3389/fnins.2019.00659.

[8] Gf Chen. "Amyloid beta: structure, biology and structure-based therapeutic development". In: *Acta Pharmacol Sin* (2017). DOI: 10.1038/aps.2017.28.

[9] "Hsimulator, Luca Marchetti University of Trento". In: (2017).

[10] L.A Demetrius. "Alzheimer's disease: The amyloid hypothesis and the Inverse Warburg effect". In: *Frontiers* (2015). DOI: 10.3389/fphys.2014.00522.

[11] Maltsev AV. "The role of -amyloid peptide in neurodegenerative diseases". In: *PupMed* (2011). DOI: 10.1016/j.arr.2011.03.002.

[12] et. al Cohen SI. "Determination of self-consistent solutions to growth processes described by nonlinear master equations". In: *J Chem Phys* (2011). DOI: 10.1063/1.3608917.

[13] et. al Cohen SI. "Nucleated polymerization with secondary pathways. I. Time evolution of the principal moments". In: *J Chem Phys* (2011). DOI: 10.1063/1.3608916.

[14] et. al Knowles T.P.J. "An Analytical Solution to the Kinetics of Breakable Filament Assembly". In: *Science* (2009). DOI: 15331537.

[15] D.T. Gillespie. "A general method for numerically simulating the stochastic time evolution of coupled chemical reactions". In: *Comput. Phy* (1976). DOI: 403434.

[16] S Oosawa F.; Asakura. "Thermodynamics of the Polymerization of Protein". In: *Academic Press* (1975).

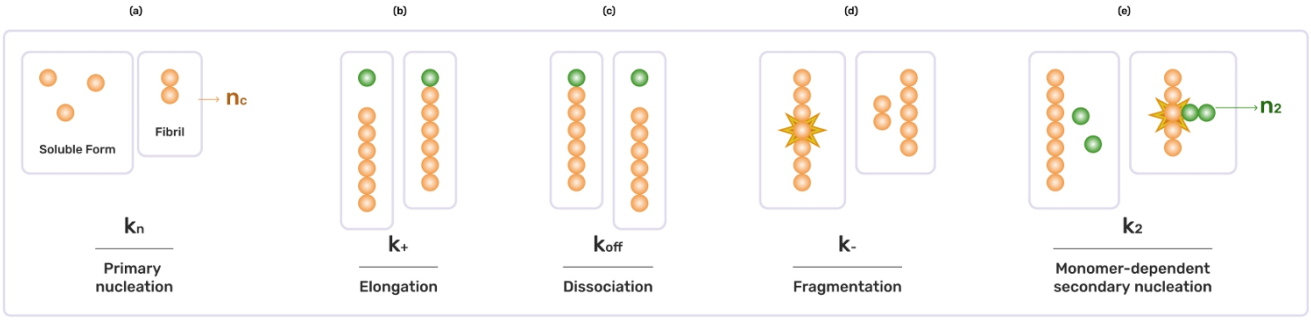

Figure 1: *Scheme illustrating the microscopic processes of polymerisation. Primary nucleation (a) leads to the creation of a polymer of length nc from soluble monomer. Filaments grow linearly (b) from both ends in a reversible manner with monomers also able to dissociate from the ends (c). The secondary pathways (d) and (e) lead to the creation of new fibril ends from pre-existing polymers; fragmentation (d) and monomer-dependent secondary nucleation (e).[1]*

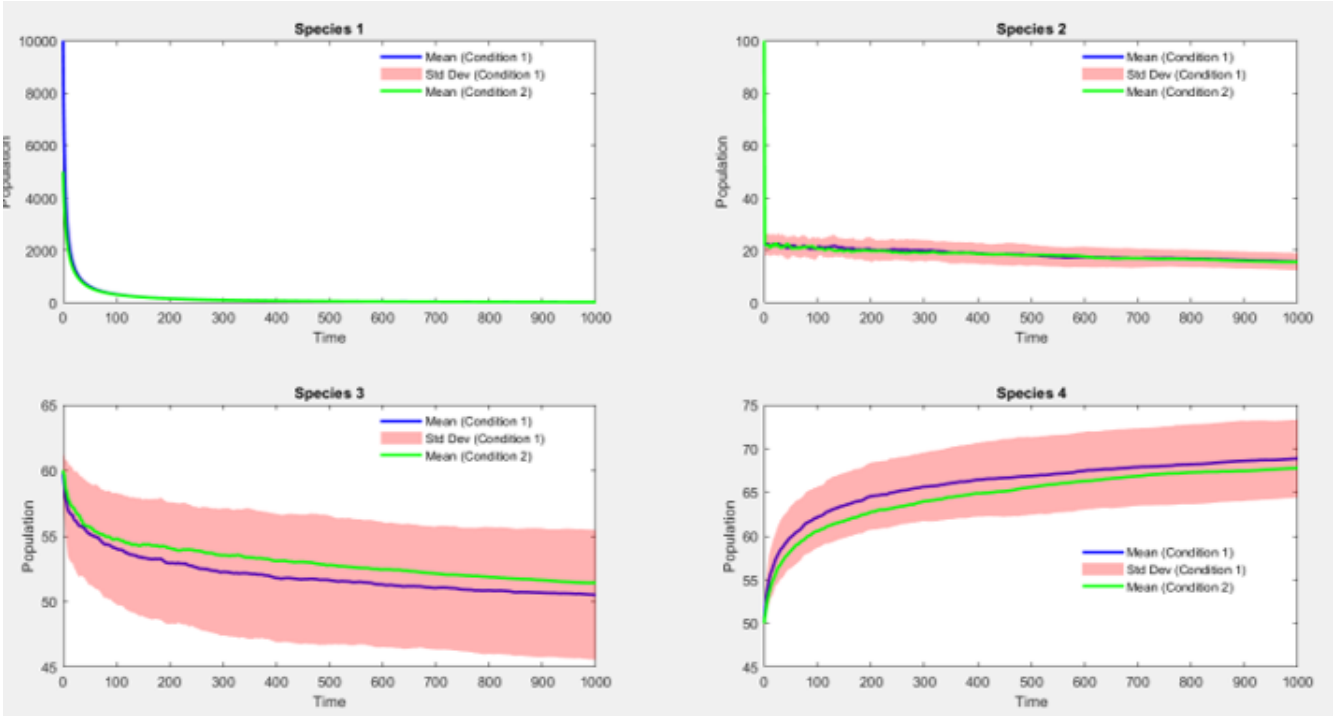

Figure 2: *The evolution of amyloid beta aggregations for M1, M2, M3 and M4. Rate constants* ($k_0 \neq \ldots \neq k_{53}$)*,* $k_0 = 0.00001$*,* $k_2 = k_0/2, \ldots$*.Condition 1* $M1 = 10000$ *and Condition 2* $M2 = 5000$*, and the other populations* $M2, \ldots, M8$ *are respectively* $100, 60, 50, 20, 10, 5, 5$

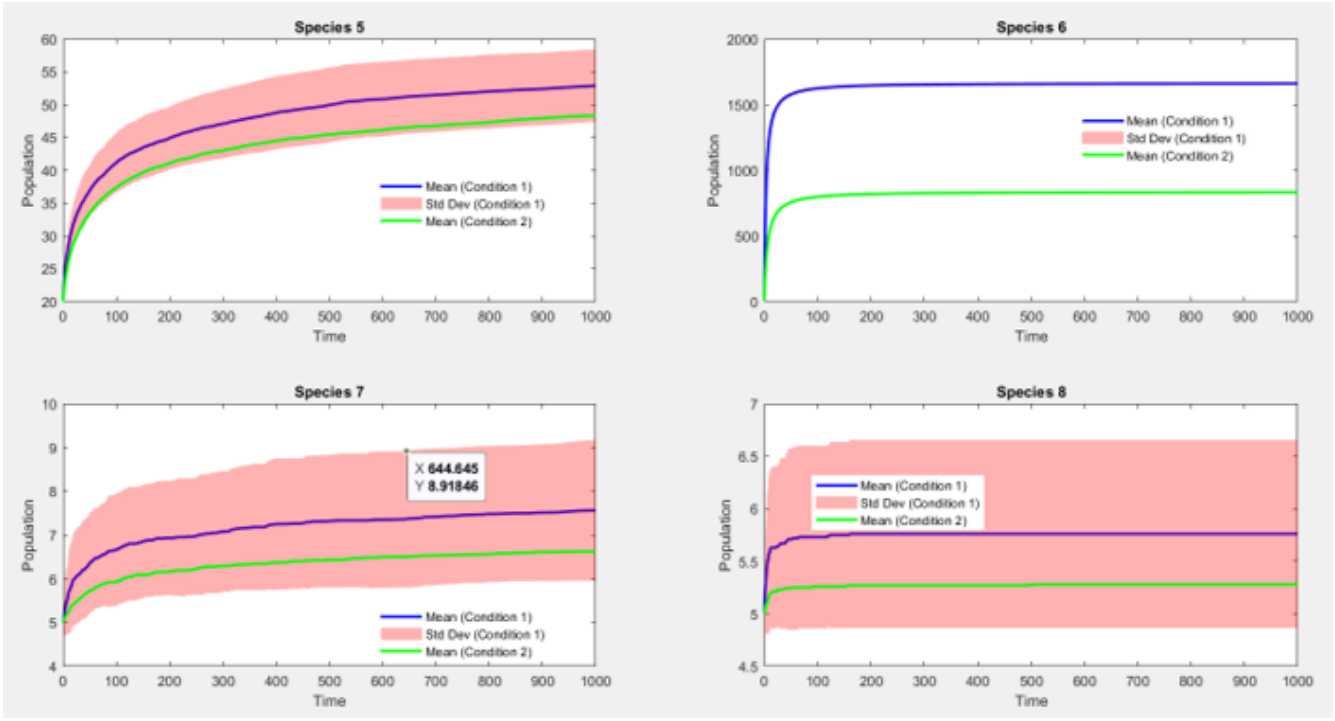

Figure 3: *The evolution of amyloid beta aggregations for M5, M6, M7 and M8. Rate constants* ($k_0 \neq \ldots \neq k_{53}$)*,* $k_0 = 0.00001$*,* $k_2 = k_0/2, \ldots$*.Condition 1* $M1 = 10000$ *and Condition 2* $M2 = 5000$*, and the other populations* $M2, \ldots, M8$ *are respectively* $100, 60, 50, 20, 10, 5, 5$

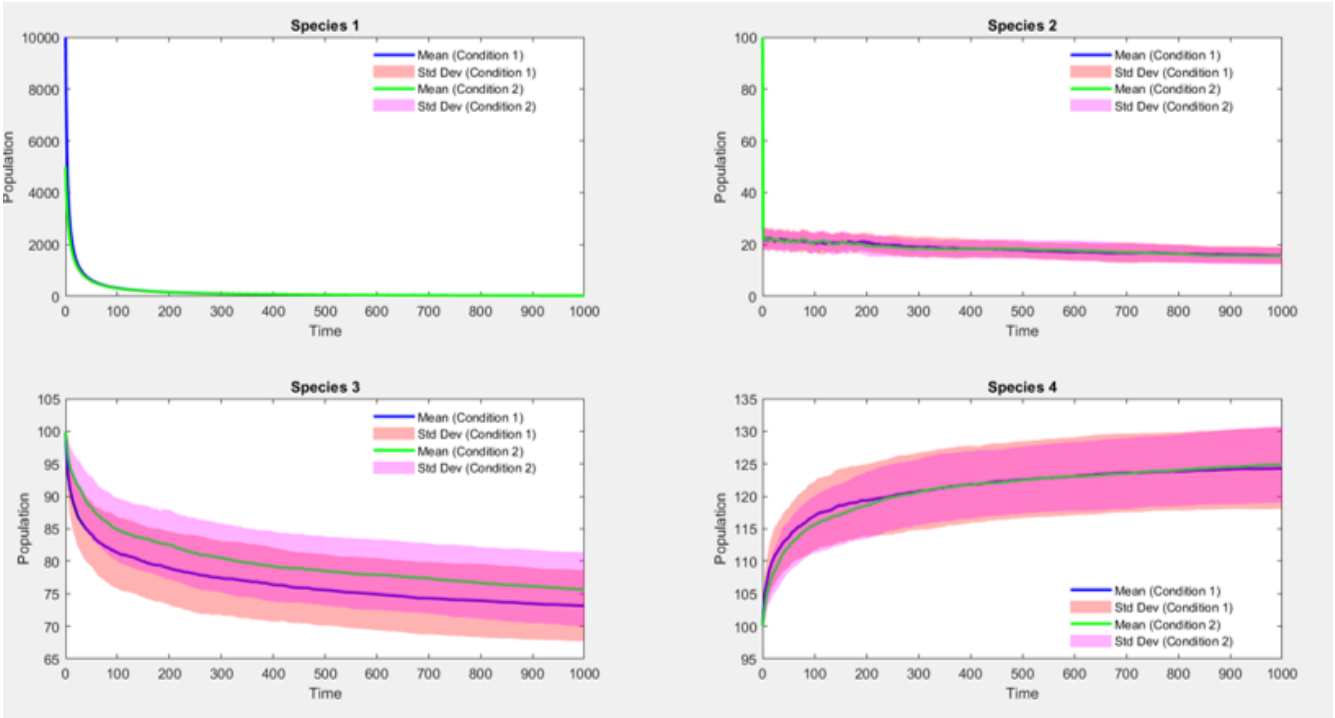

Figure 4: *The evolution of amyloid beta aggregations and fragmentation for M1, M2, M3 and M4. Rate constants* ($k_0 \neq \ldots \neq k_{53}$)*,* $k_0 = 0.00001$*,* $k_2 = k_0/2, \ldots$*.Condition 1* $M1 = 10000$ *and Condition 2* $M2 = 5000$*, and the other populations* $M2, \ldots, M8 = 100$

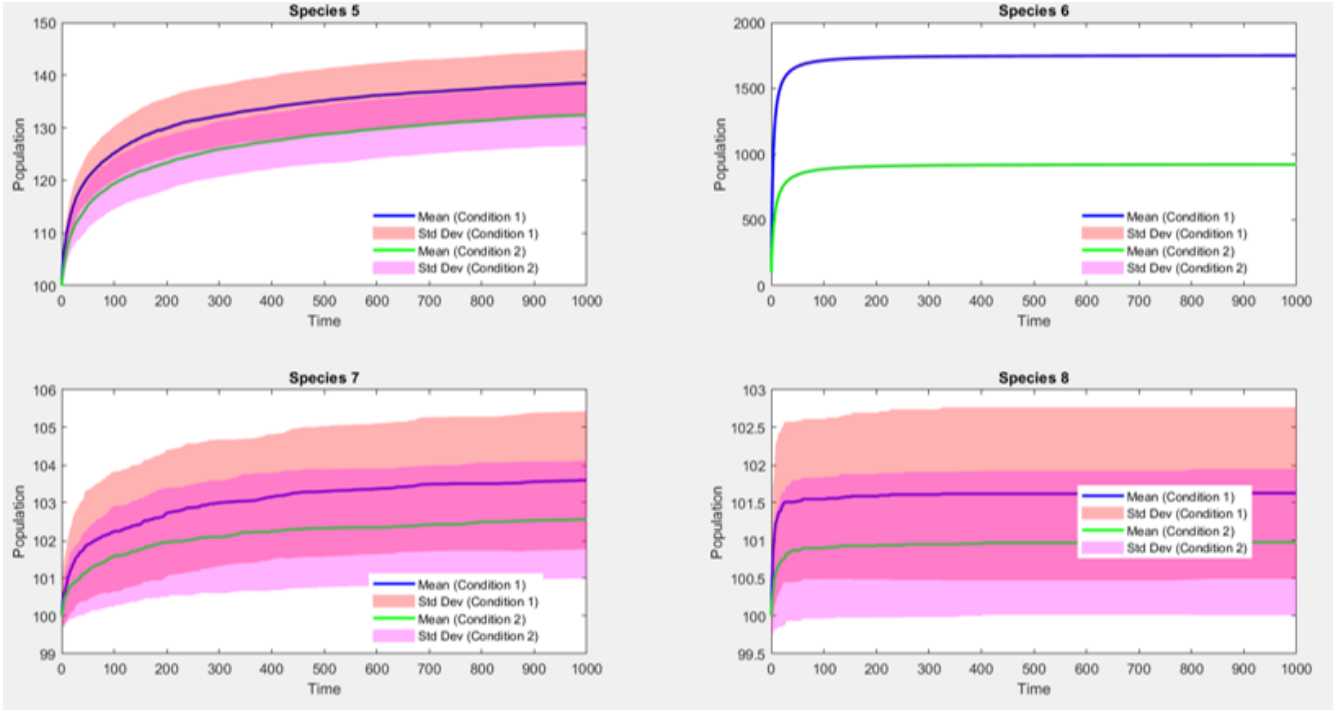

Figure 5: *The evolution of amyloid beta aggregations and fragmentation for M5, M6, M7 and M8. Rate constants* ($k_0 \neq \ldots \neq k_{53}$)*,* $k_0 = 0.00001$*,* $k_2 = k_0/2, \ldots$*.Condition 1* $M1 = 10000$ *and Condition 2* $M2 = 5000$*, and the other populations* $M2, \ldots, M8 = 100$

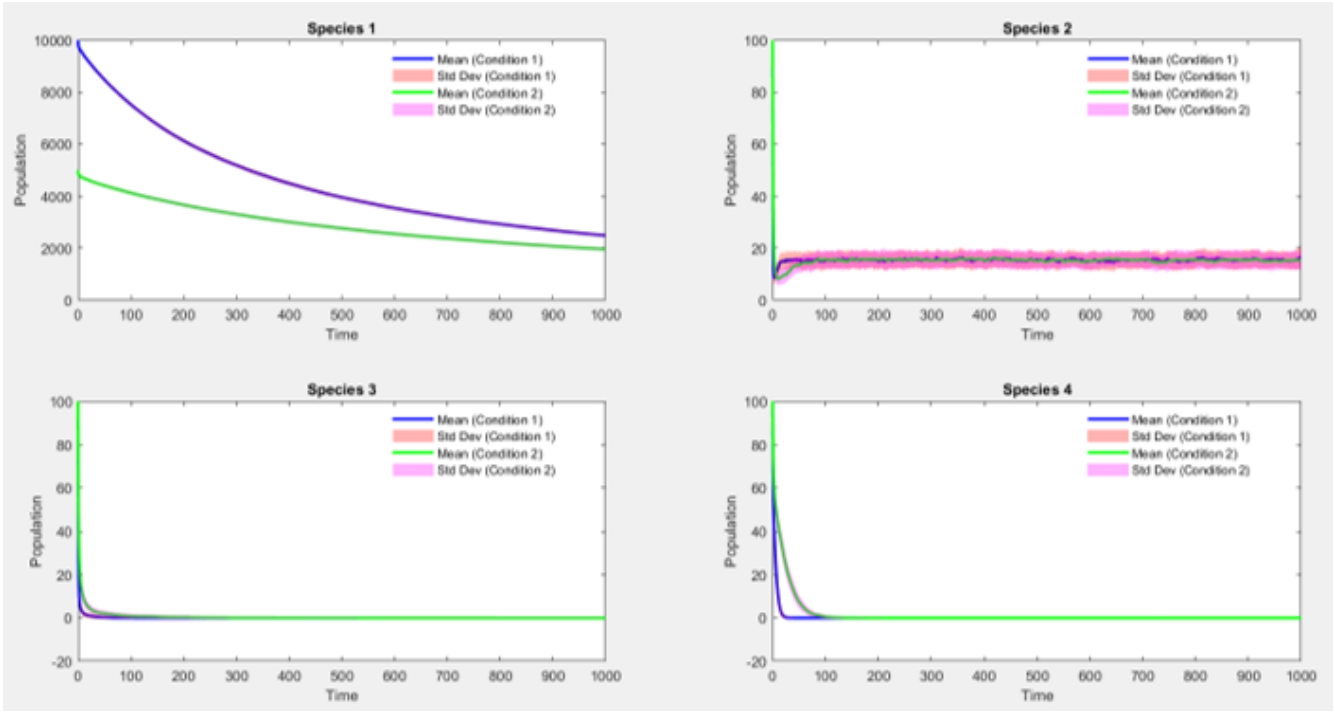

Figure 6: *The evolution of amyloid beta aggregations and fragmentation for M1, M2, M3 and M4. Rate constants for each reaction* ($k_0 \neq \ldots \neq k_{53}$)*, setting* $k_0 = 0.00001$*,* $k_2 = k_0/2, \ldots$*, testing two initial populations of free protein* $M1 = 10000$ *and* $M1 = 5000$*, and the other populations* $M2, \ldots, M8 = 100$

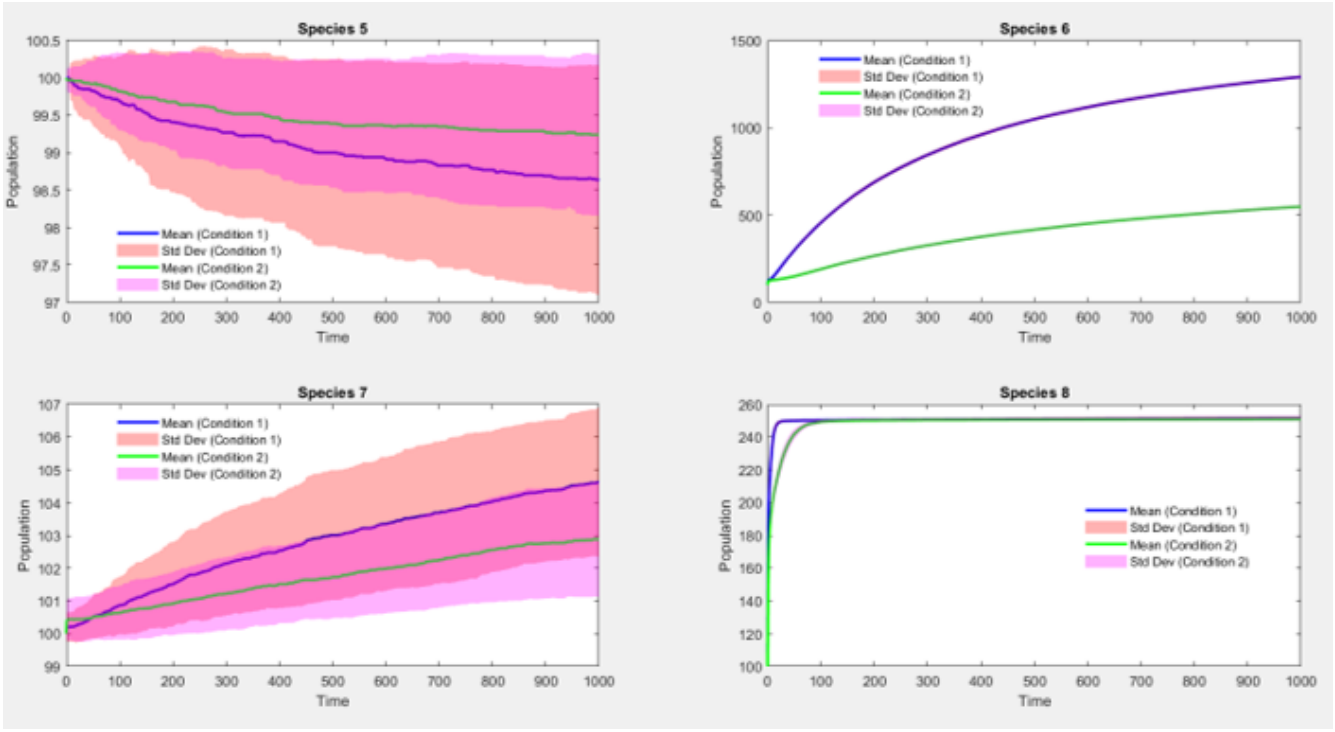

Figure 7: *The evolution of amyloid beta aggregations and fragmentation for M5, M6, M7 and M8. Rate constants for each reaction ($k_0 \neq \ldots \neq k_{53}$), setting $k_0 = 0.00001$, $k_2 = k_0/2, \ldots$, testing two initial populations of free protein $M1 = 10000$ and $M1 = 5000$, and the other populations $M2, \ldots, M8 = 100$*

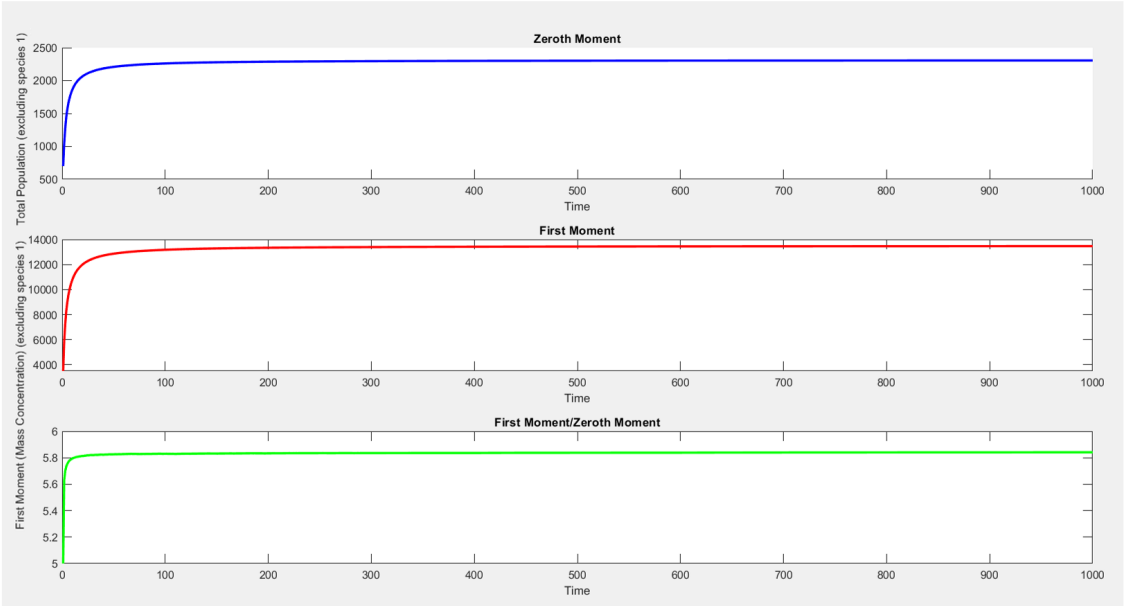

Figure 8: *Zero and First moment with the same condition (3)*

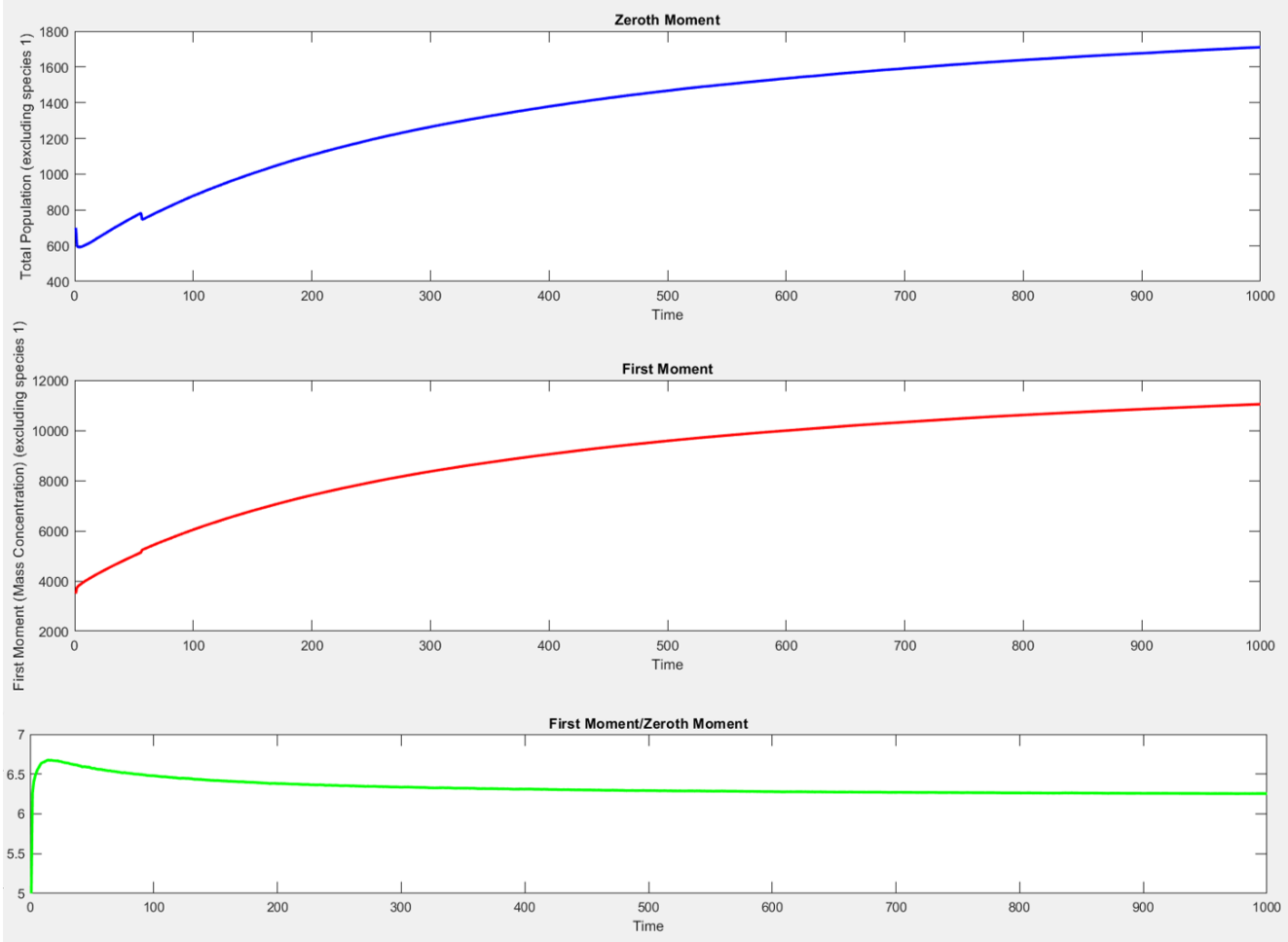

Figure 9: *Zero and First moment with the same condition (5)*

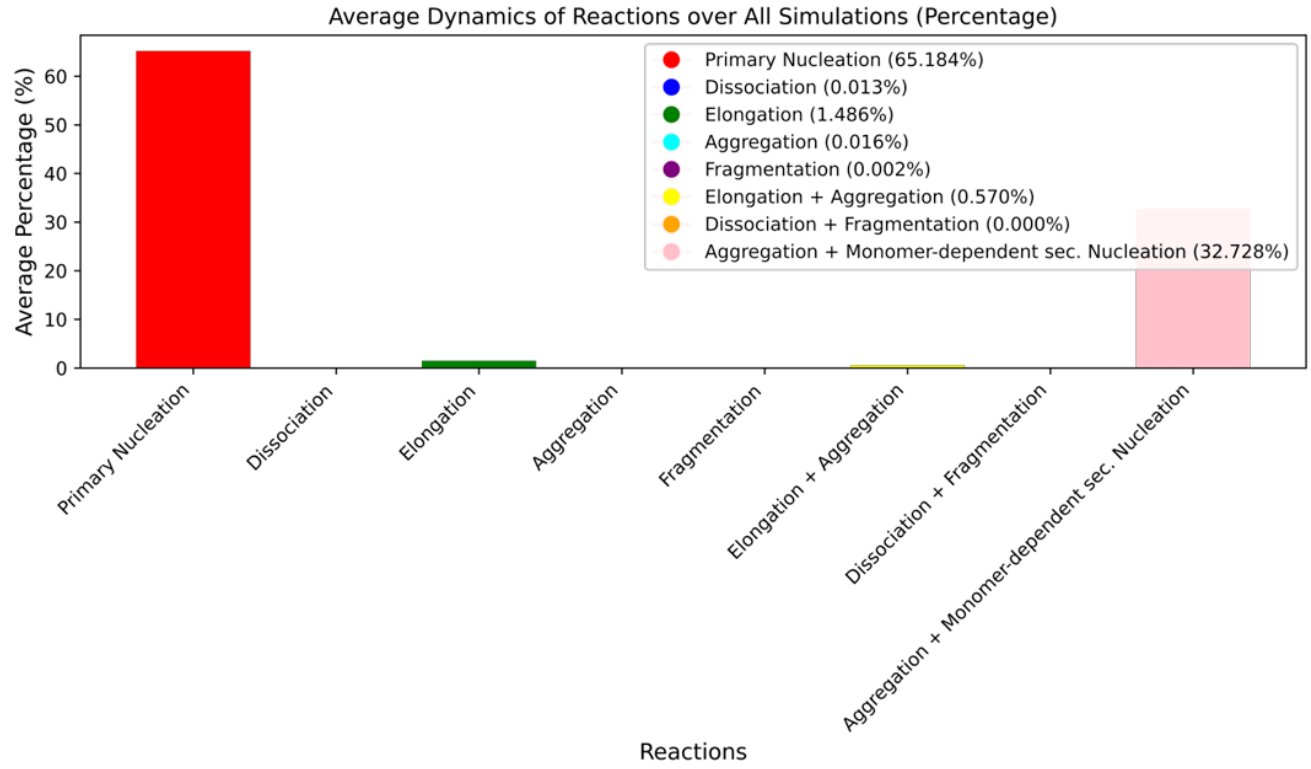

Figure 10: *The evolution of amyloid-beta aggregations and fragmentation events and their occurrence dynamics with different initial conditions and reaction rates. The average reaction dynamics corresponding to condition 3), with M1 = 10,000 and M2,..., M8 = 100.*

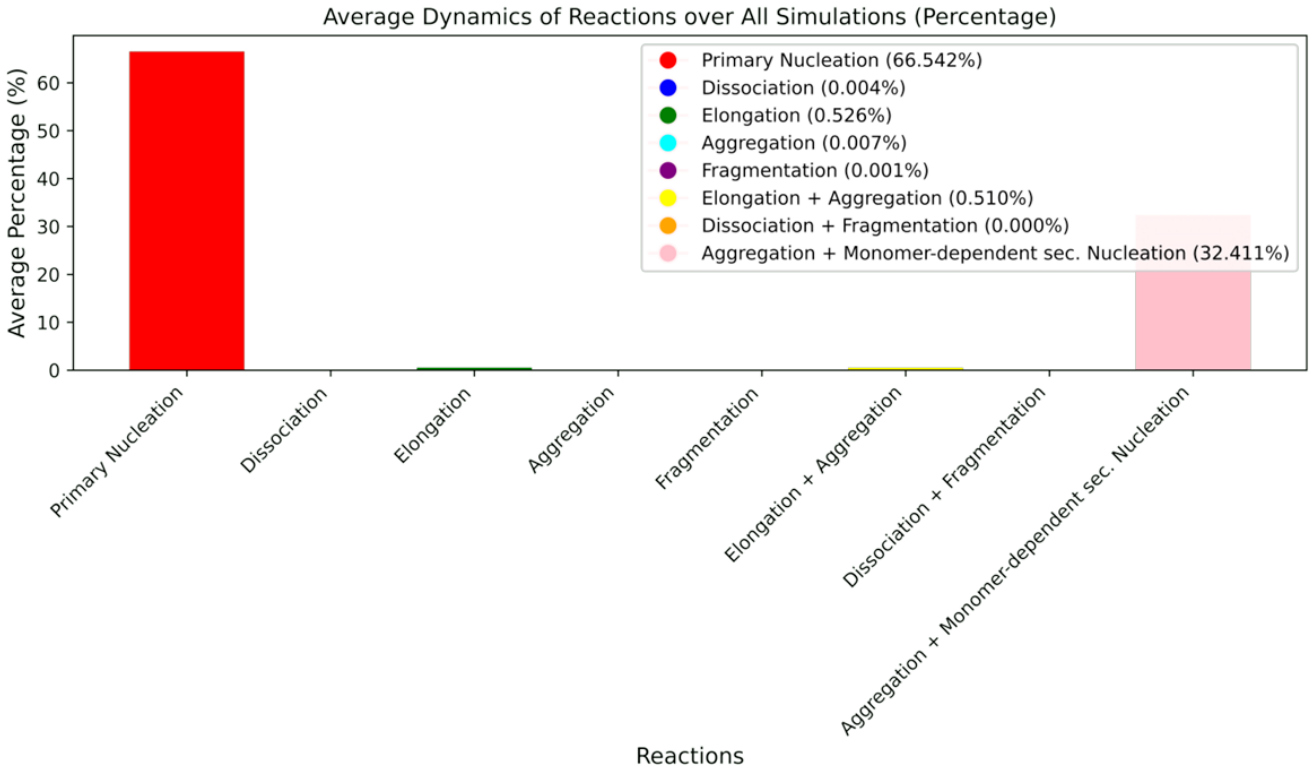

Figure 11: *The evolution of amyloid-beta aggregations and fragmentation events and their occurrence dynamics with different initial conditions and reaction rates. The average reaction dynamics with M1 = 10000 and M2,..., M8 = 1 and random switching with dynamic constant rates as in condition 4.*

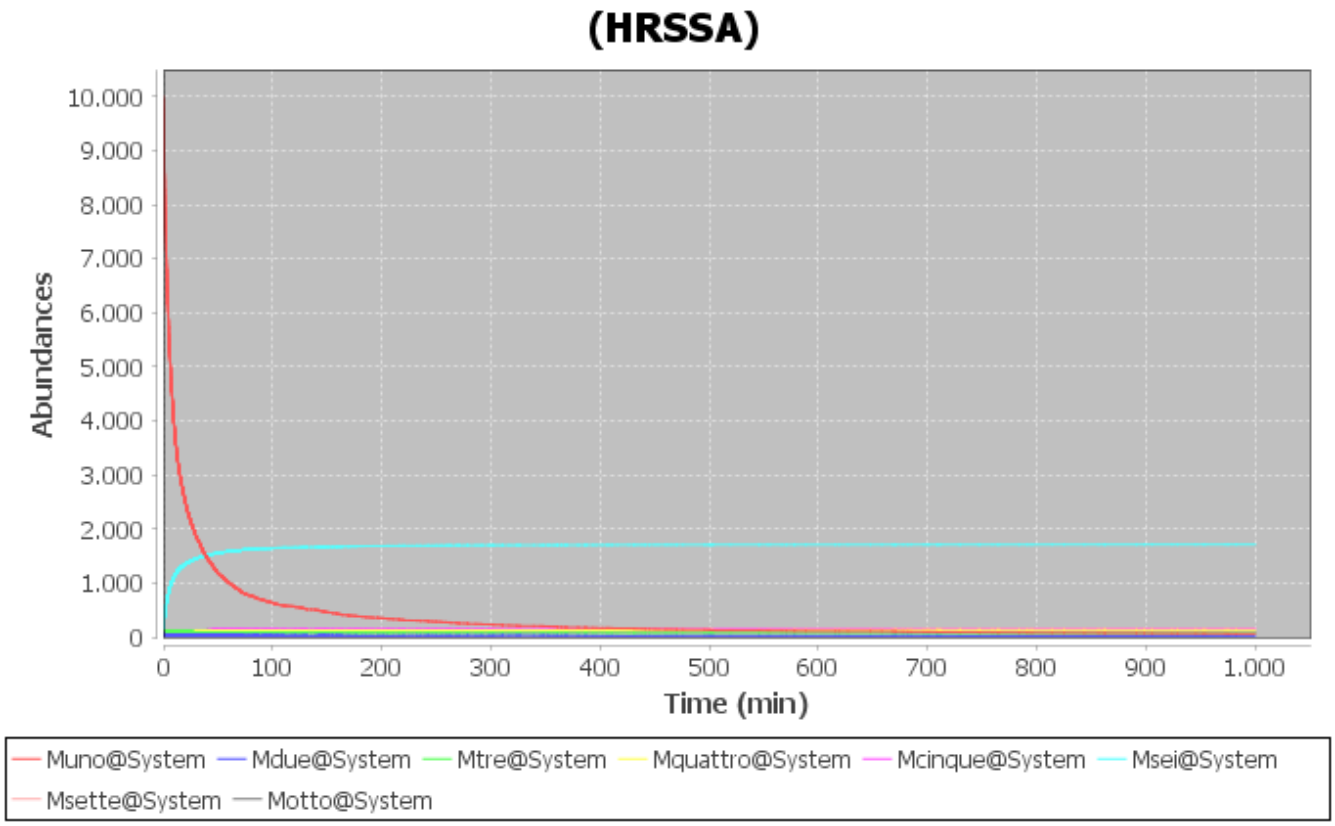

Figure 12: *Simulation with HRSSA method when the rate constants are different for reactions, and initial conditions* $M_1 = 10000$*,* $M_2, M_3, M_4, M_5, M_6, M_7, M_8 = 100$*. The starting reaction rate* $k_0 = 0.00001$ *for aggregation and starting rate for fragmentation* $k_1 = 0.00001/2$*.*

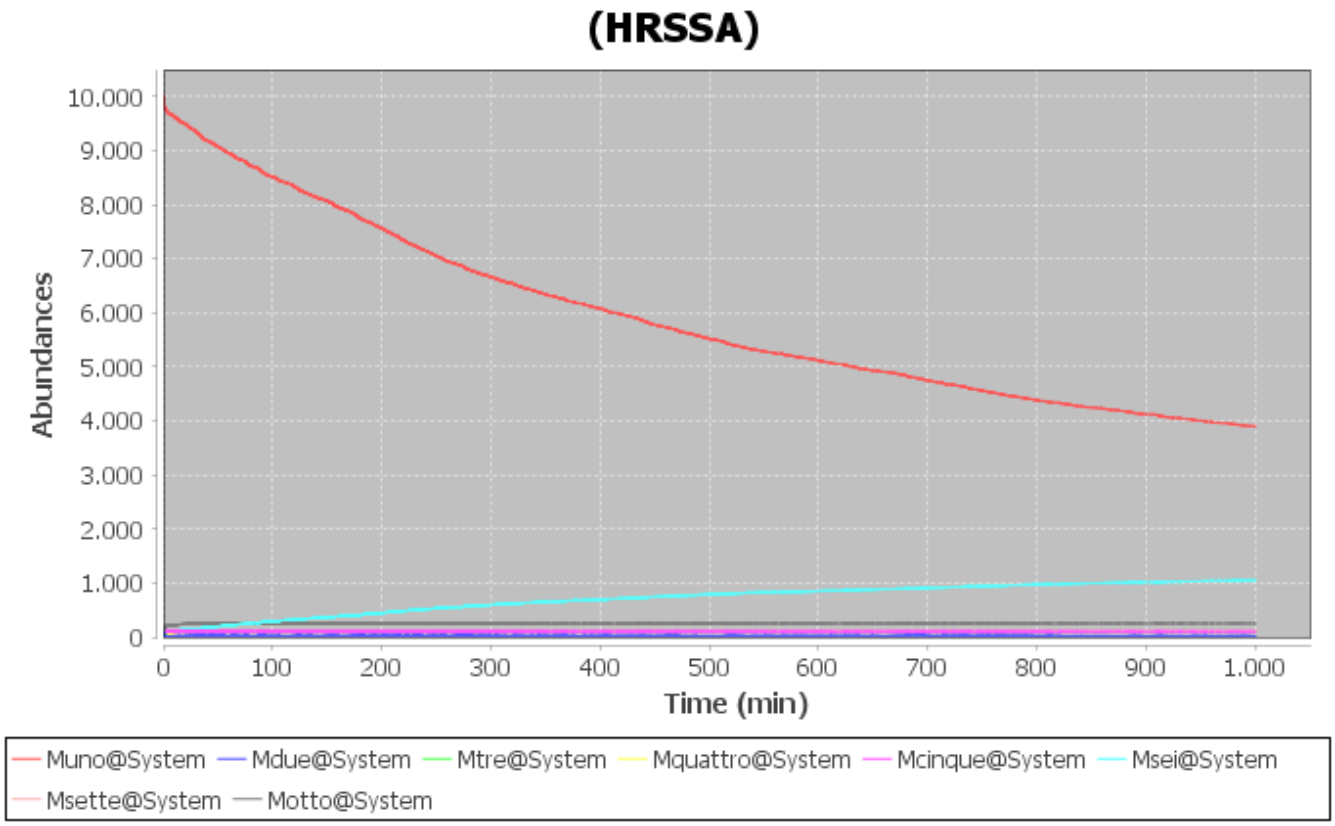

Figure 13: *Simulation with HRSSA method when the rate constants are constant for all reactions except from* $k_0 = 0.0000001$, *e.g.,* $k_1, ..., k_{26} = 0.0000000002$ *and* $k_{27}, ..., k_{53} = 0000000002/2$; *initial population of free proteins* $M_1 = 10000$, *and* $M_2, M_3, M_4, M_5, M_6, M_7, M_8 = 100$.